310
4/23
UC-25 & Fast Reactor
CFTI

1338

AI-AEC-12932

MASTER

EFFECT OF HELIUM ON STRESS–RUPTURE BEHAVIOR OF TYPES 304 AND 316 STAINLESS STEELS

AEC Research and Development Report

Atomics International
North American Rockwell

P.O. Box 309
Canoga Park, California 91304

DISCLAIMER

Printed in the United States of America
Available from
Clearinghouse for Federal Scientific and Technical Information
National Bureau of Standards, U.S. Department of Commerce
Springfield, Virginia 22151
Price: Printed Copy $3.00; Microfiche $0.65

AI-AEC-12932
METALS, CERAMICS
AND MATERIALS

EFFECT OF HELIUM ON STRESS–RUPTURE BEHAVIOR OF TYPES 304 AND 316 STAINLESS STEELS

By:
K. R. GARR
D. KRAMER
C. G. RHODES*

*North American Rockwell Science Center

Atomics International
North American Rockwell
P.O. Box 309
Canoga Park, California 91304

CONTRACT: AT(04–3)–701
ISSUED: APRIL 15, 1970

DISTRIBUTION

This report has been distributed according to the category "Metals, Ceramics, and Materials" as given in the Standard Distribution for Unclassified Scientific and Technical Reports, TID-4500.

ACKNOWLEDGMENT

The authors are grateful to R. M. Kniefel and K. G. Clody for assistance with the cyclotron injection and stress-rupture testing of the samples, and to R. A. Spurling for some of the light and electron microscopy. The helium analysis was performed by H. Farrar IV.

CONTENTS

	Page
Abstract	6
I. Introduction	7
II. Experimental	8
A. Materials	8
B. Heat Treatments and Initial Microstructure	8
C. Testing	9
D. Strain Analysis	9
III. Results	11
A. Stress-Rupture Tests	11
B. Metallography	13
1. Light Microscopy	13
2. Replica Electron Microscopy	17
3. Thin Foil Electron Microscopy	17
C. Strain Analysis	18
IV. Discussion	24
V. Conclusions	24
References	28

TABLES

1. Composition of the Alloys	8
2. Heat Treatments of Alloys	9
3. Comparison of Elongations Observed During Stress-Rupture and Tensile Testing	13
4. Summary of Metallography for Stress Rupture of Types 304 and 316 Stainless Steels Tested at 760 and 700°C, Respectively	14
5. Summary of Strain Analysis on Stress-Rupture Samples of Type 316 Stainless Steel Given Heat Treatment No. 6 and Tested at 700°C	18

FIGURES

Page

1. Stress Rupture of Type 304 Stainless Steel Tested in Vacuum at 760°C 12
2. Stress Rupture of Type 316 Stainless Steel Tested in Vacuum at 700°C 12
3. Type 304 Stainless Steel Tested at 760°C (Note increase in amount of intergranular cracking in helium-containing samples)
   a. No Helium, Rupture Life = 511 hr, Elongation = 38% 15
   b. 1.5×10^{-6} atom fraction Helium, Rupture Life = 419 hr, Elongation = 17% 15
   c. 3.5×10^{-5} atom fraction Helium, Rupture Life = 325 hr, Elongation = 11% 15
4. Type 316 Stainless Steel (Treatment 6) Tested at 700°C (Note increased intergranular cracking and lack of grain distortion in helium-containing sample, compared to control)
   a. No Helium, Rupture Life = 1075 hr, Elongation = 44% 15
   b. 4.0×10^{-5} atom fraction Helium, Rupture Life = 594 hr, Elongation = 10% 15
5. Type 316 Stainless Steel (Treatment 13) Tested at 700°C (Note increase in intergranular cracking in helium-containing samples, and increased amount of multifaceted cracks in c., compared to b.)
   a. No Helium, Rupture Life = 683 hr, Elongation = 5% 15
   b. 4.0×10^{-5} atom fraction Helium, Rupture Life = 173 hr, Elongation = 2% 15
   c. 4.0×10^{-5} atom fraction Helium, Rupture Life = 401 hr, Elongation = 1% 15
6. Type 316 Stainless Steel (Treatment 6) Tested at 700°C (Note increase in voids on grain boundaries of helium-containing sample over control)
   a. No Helium, Rupture Life = 1075 hr, Elongation = 44% 16
   b. 4.0×10^{-5} atom fraction Helium, Rupture Life = 316 hr, Elongation = 13% 16
7. Type 316 Stainless Steel (Treatment 13) Tested at 700°C (Note increase in voids on grain boundaries of helium-containing sample)
   a. No Helium, Rupture Life = 683 hr, Elongation = 5% 19
   b. 4.0×10^{-5} atom fraction Helium, Rupture Life = 173 hr, Elongation = 2% 19

FIGURES

Page

8. Type 304 Stainless Steel Tested at 760°C (Largest helium bubbles are generally in carbide-matrix interface)
   a. 1.5×10^{-6} atom fraction Helium, Rupture Life = 419 hr, Elongation = 17% 20
   b. 3.5×10^{-5} atom fraction Helium, Rupture Life = 325 hr, Elongation = 11% 20
9. Type 316 Stainless Steel (Treatment 6) Containing 4.0×10^{-5} atom fraction Helium, Tested at 700°C, Showing Helium Bubbles in Grain Boundary. Rupture Life = 316 hr, Elongation = 13%. 21
10. Type 316 Stainless Steel (Treatment 6) Containing 4.0×10^{-5} atom fraction Helium, Tested at 700°C, Showing Growth of Sigma Phase on $M_{23}C_6$ Particle. Rupture Life = 594 hr, Elongation = 10% 21
11. Type 316 Stainless Steel (Treatment 13) Containing 4.0×10^{-5} atom fraction Helium, Tested at 700°C, Showing Helium Bubbles in Matrix and in Prior Slip and Deformation Bands. Rupture Life = 173 hr, Elongation = 2% 21
12. Type 316 Stainless Steel (Treatment 6) Tested at 700°C (Note lack of polygonization in helium-containing sample)
    a. No Helium, Rupture Life = 1075 hr, Elongation = 44%. 22
    b. 4.0×10^{-5} atom fraction Helium, Rupture Life = 316 hr, Elongation = 13% 22

ABSTRACT

Flat tensile samples of Types 304 and 316 stainless steels, with helium contents of 1.5×10^{-6} and either 3.5 or 4.0×10^{-5} atom fraction, were stress-rupture tested in vacuum at 760°C (Type 304) and 700°C (Type 316). The presence of helium caused large reductions in rupture life and in elongation at failure. The amount of strain produced within the grains of helium-containing samples was a small fraction of the measured total elongation. The difference in these values was accounted for by extensive intergranular cracking.

I. INTRODUCTION

Stainless steel is susceptible to helium embrittlement when exposed to a fast-neutron flux at elevated temperatures, such as a fuel cladding would experience during Liquid Metal Cooled Fast Breeder Reactor (LMFBR) service. The helium is produced uniformly on a microscopic scale by an (n, α) reaction involving the major alloy constituents. The embrittling effect of helium results from its tendency to concentrate at grain boundaries, which leads to premature intergranular cracking.

The effect of helium on the tensile properties of Types 304 and 316 stainless steels[1,2] has been previously investigated by injecting helium into samples, using α-particle irradiation from a cyclotron. This method makes it possible to study helium embrittlement without resorting to lengthy reactor irradiations. The present investigation is an extension of this work to the effects of helium on the stress-rupture behavior of these austenitic stainless steels.

II. EXPERIMENTAL

A. MATERIALS

Samples (0.009 by 0.040 in., with a gauge length of 0.500 in.) of Types 304 and 316 stainless steels were fabricated from sheet stock, and irradiated with α particles at the University of Washington's cyclotron. The details of the irradiation technique have been reported earlier.[1] The compositions of the two alloys are given in Table 1.

TABLE 1
COMPOSITION OF THE ALLOYS
(wt %)

Alloy	Constituent							
	Fe	Cr	Ni	Mn	Mo	N	C	B
Type 304	bal	18.8	9.3	1.6	0.25	0.06	0.05	0.0009
Type 316	bal	17.3	13.6	*	2.3	0.05	0.06	*

*Undetermined

The helium concentrations, as determined by mass spectrometry using an isotopic dilution method,[3] were 1.5×10^{-6} and 3.5×10^{-5} atom fraction helium in the Type 304 samples and 1.5×10^{-6} and 4.0×10^{-5} atom fraction helium in the Type 316 samples.

B. HEAT TREATMENTS AND INITIAL MICROSTRUCTURE

Heat treatments given the alloys prior to irradiation are shown in Table 2. Samples of Types 304 and 316 given Treatment 6 have essentially the same initial microstructure, consisting of austenitic grains, 27 and 40 μ in size, with $M_{23}C_6$ carbides on the grain boundaries. The Type 316 samples given Treatment 13 had a grain size of $\sim$100 μ. Recrystallization did not take place during the duplex aging treatment, but precipitation occurred within the grains, in the slip and deformation bands, and in the grain boundaries.

The precipitates within the grains were identified by electron diffraction techniques as σ, whereas the precipitates in the grain boundaries were primarily $M_{23}C_6$ with some σ present;[2] ϵ-martensite was also detected within the grains.

TABLE 2

HEAT TREATMENTS OF ALLOYS

Alloy	Treatment
Type 304	5 hr at 1010°C + 100 hr at 760°C
Type 316	1 hr at 982°C + 8 hr at 760°C (Treatment 6)
	30 min at 1120°C → 25% CR* → 24 hr at 482°C + 194 hr at 704°C (Treatment 13)

*CR — Cold-rolling

C. TESTING

All stress-rupture tests were done in vacuum ($\sim 4 \times 10^{-6}$ Torr). The samples were dead loaded after being heated to the desired test temperature and held for 1 hr. The sample temperature was maintained within ±3°C, and the time to rupture was recorded on an electric clock which was automatically turned off when the sample broke.

The strain at rupture was determined after testing by using a traveling microscope to measure the increase in overall length of the sample and then dividing this increase by the original gauge length. Two measurements were made on each sample, with the microscope traveling in opposite directions. The average length obtained was used for the computation. In making the measurements, the largest error (<2%) arises in reproducing the same position at the fracture edge on each section of the sample.

D. STRAIN ANALYSIS

The strain which took place within the grains of the tested samples was calculated by use of an equation originally derived by Rachinger.[4] Hensler and Gifkins[5] have recently improved on the data collection method. In both cases, the grains were assumed to be equiaxed prior to testing. In the present investigation, we followed Rachinger's original thesis, but did not make the assumption of initially equiaxed grains ($w/\ell = 1$). The result is

$$E_g = (\langle L/W \rangle)^{2/3} \, (\langle w/\ell \rangle)^{2/3} - 1 \qquad \ldots (1)$$

where we have also applied the method of Hensler and Gifkins. In Equation 1, E_g is the slip strain within the grains, ℓ and L are the length of the grains measured parallel to the tensile axis in an untested and tested sample, respectively, and w and W are the width of the grains measured perpendicular to the tensile axis in an untested and tested sample, respectively. The grains are measured at their respective maxima, and the required ratio computed for each individual grain. The ratio is then summed, and the average value calculated for use in Equation 1. The confidence limits on E_g are obtained from the standard formula:[6]

$$-Z_{\alpha/2}\sigma_{E_g}\Big/\sqrt{N} \leq E_g \leq +Z_{\alpha/2}\sigma_{E_g}\Big/\sqrt{N} \qquad \ldots (2)$$

In Equation 2, $Z_{\alpha/2}$ is the two-tailed Z statistic with confidence limit α, and N is the number of samples used in the analysis. σ_{E_g} is the sample data standard of deviation, given by:[7]

$$\sigma_{E_g} = \left\{\left[\frac{\partial E_g}{\partial(\langle L/W\rangle)}\right]^2 \sigma_1^2 + \left[\frac{\partial E_g}{\partial(\langle w/\ell\rangle)}\right]^2 \sigma_2^2\right\}^{1/2} , \qquad \ldots (3)$$

where σ_1 and σ_2 are the sample data standard of deviation for the computed ratios (L/W) and (w/ℓ), respectively. The dimensions of the grains were obtained from enlargements (8 x 10) of photomicrographs, using a Bausch and Lomb 7 X measuring magnifier (least reading, 0.01 mm). Seventy grains in each sample were measured.

III. RESULTS

A. STRESS-RUPTURE TESTS

Figure 1 is a plot of the initial stress vs the rupture life for Type 304 stainless steel tested at 760°C. The lines are drawn according to a least squares fit of the data, assuming an equation of the type:

$$\log \sigma = a + b \log t_r \quad , \qquad \ldots (4)$$

where σ is the initial stress, t_r is the rupture life, and a and b are constants.

We have analyzed all the data for the helium-containing samples as a single group. The resulting straight line, shown in Figure 1, is a good fit to the data. From this analysis, it appears that the reduction in rupture life due to helium is decreasing as the initial stress is decreased. Also, the effect is independent of the helium concentration, within the range of stresses and helium concentrations used in the present study.

Figure 2 is a plot of the initial stress vs the rupture life for Type 316 stainless steel tested at 700°C. The lines are drawn according to the least squares analysis, using Equation 4. Samples given Treatment 6 show slightly larger reductions in rupture life as the initial stress is decreased. Again, the data for the helium-containing samples have been analyzed as a group, regardless of concentration. As in the case of Type 304, the reduction in rupture life appears to be independent of the helium concentration.

Samples given Treatment 13 exhibit an effect of helium concentration on rupture life. Those containing 1.5×10^{-6} atom fraction helium exhibit a strong reduction in rupture life, for times greater than ~125 hr, as the initial stress is decreased. Samples with 4.0×10^{-5} atom fraction helium have a rupture life reduced by a factor of ~4 at the shorter times (<200 hr); whereas, at longer times, the loss in rupture life appears to be considerably greater. This assumes that the control samples exhibit a behavior in rupture life which is an extrapolation of that shown in Figure 2.

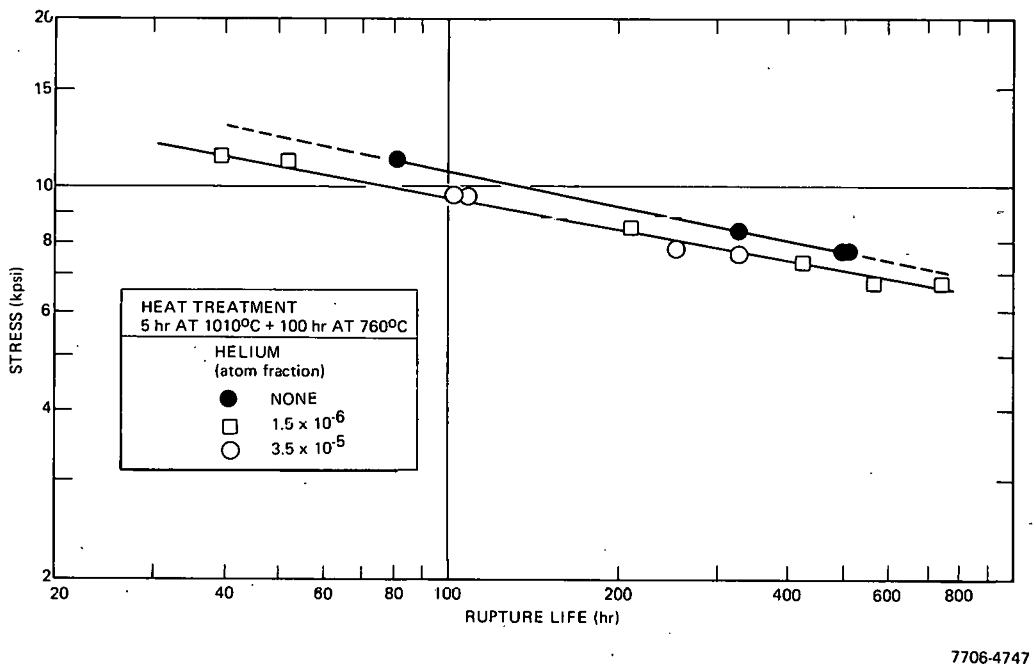

Figure 1. Stress Rupture of Type 304 Stainless Steel Tested in Vacuum at 760°C

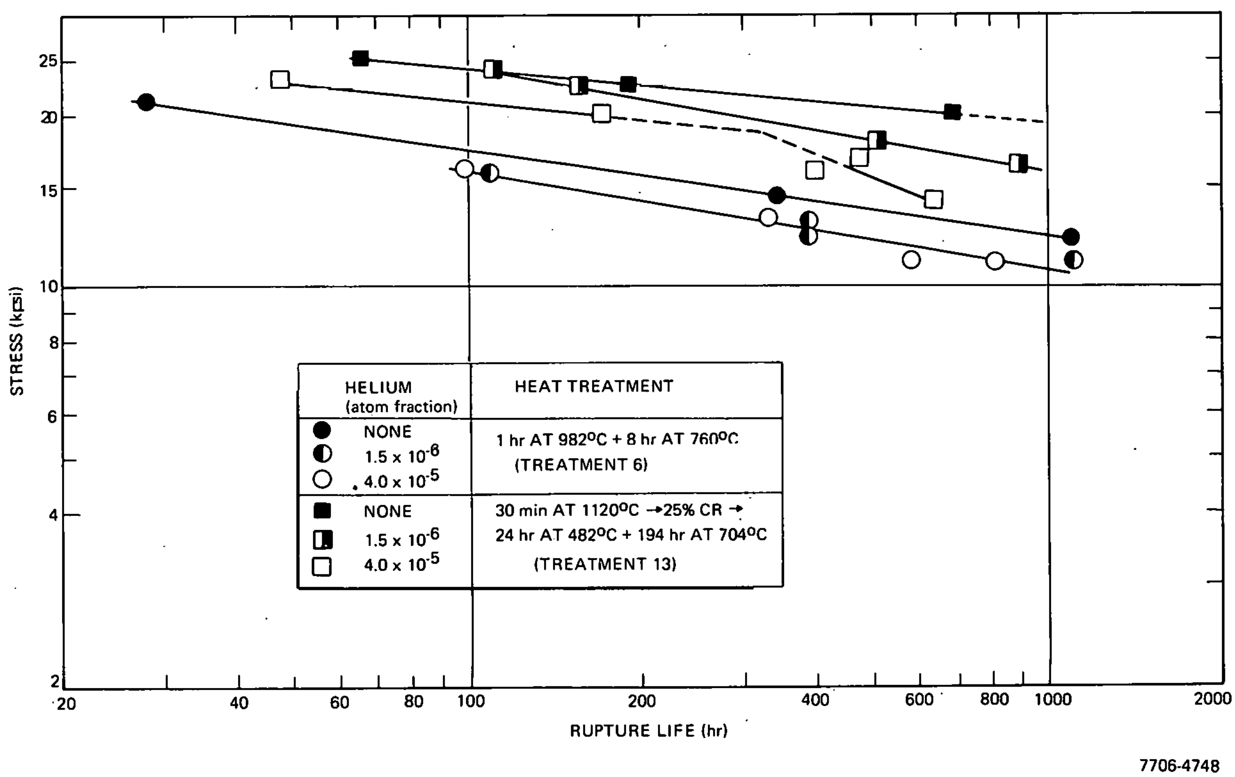

Figure 2. Stress Rupture of Type 316 Stainless Steel Tested in Vacuum at 700°C

The range of elongations at rupture for all samples are given in Table 3, along with previous tensile data.[1,2] Samples of Type 316 (Treatment 13) with helium exhibit a much smaller elongation than their tensile-tested counterparts. Otherwise, elongations of the stress-rupture samples are comparable to those of the tensile-tested samples.

TABLE 3

COMPARISON OF ELONGATIONS OBSERVED DURING STRESS-RUPTURE AND TENSILE TESTING

Alloy	Test Tempera-ture (°C)	Helium (atom fraction)	Elongation in Stress Rupture (%)		Elongation in Tensile Test Average Value (%)
			Minimum	Maximum	
Type 304	760	0	27	46	42
		1.5×10^{-6}	16	24	-
		3.5×10^{-5}	11	14	14
Type 316 Treatment 6	700	0	41	52	46
		1.5×10^{-6}	13	24	21
		4.0×10^{-5}	10	13	14
Type 316 Treat-ment 13	700	0	5	13	11
		1.5×10^{-6}	0.9	4	9
		4.0×10^{-5}	0.5	2	8

B. METALLOGRAPHY

1. Light Microscopy

Table 4 summarizes many of the metallographic observations. Figures 3, 4, and 5 are light photomicrographs of tested samples with and without helium. The main points to note in all cases are: (1) the amount of intergranular cracking, and (2) the shape of the grains in the control and the helium-containing samples. In control samples of Types 304 and 316 (Treatment 6), the grains are elongated, as compared to the respective helium-containing samples. The amount of intergranular cracking is small in the control samples, and increases with helium concentration, as seen in Figure 3. Cracking in the helium-containing samples extends over the whole gauge length; whereas, in the control samples, it occurs only in the fracture region.

TABLE 4

SUMMARY OF METALLOGRAPHY FOR STRESS RUPTURE OF TYPES 304 AND 316 STAINLESS STEELS TESTED AT 760 AND 700°C, RESPECTIVELY

Material	Treatment	Sample Number	Helium (atom fraction)	Rupture Life (hr)	Failure Mode*	Cracking†		Polygonization in Fracture Region	New Precipitates	Bubbles		
						Fracture Region Only	Along Gauge Length			Average Size in Matrix (Å)	Density in Matrix (number/cc)	Average Size at Grain Boundary (Å)
Type 304		550	0	511	I	L		Yes	No			
		5-54	1.5×10^{-6}	419	I		M	Yes	No	40	§	100
		7-17	3.5×10^{-5}	325	I		M	Yes	No	100	2×10^{14}	200
Type 316	6	587	0	1075	T			Yes	σ and **			
	6	9-15	4.0×10^{-5}	316	I		H	Yes	No	85	4×10^{14}	120
	6	9-72	4.0×10^{-5}	594	M (I)		H	No	σ	None		None
	6	9-5	4.0×10^{-5}	817	M (I)	L		No	Yes**	§	§	§
Type 316	13	612	0	683	M	L		Yes	**			
	13	9-59	4.0×10^{-5}	173	M		H		**	45	1×10^{15}	45
	13	9-9	4.0×10^{-5}	401	M (I)		H	No	**	45	5×10^{14}	45

*T = transgranular, I = intergranular, M (I) = mostly intergranular
†L = few cracks, M = moderate density of cracks, H = high density of cracks
§Density too low for a meaningful determination
**Unable to determine

SN 1906

a. No Helium, Rupture Life = 511 hr, Elongation = 38%

SN 1997

b. 1.5×10^{-6} atom fraction Helium, Rupture Life = 419 hr, Elongation = 17%

SN 1907

c. 3.5×10^{-5} atom fraction Helium, Rupture Life = 325 hr, Elongation = 11%

Figure 3.

Type 304 Stainless Steel Tested at 760°C (Note increase in amount of intergranular cracking in helium-containing samples)

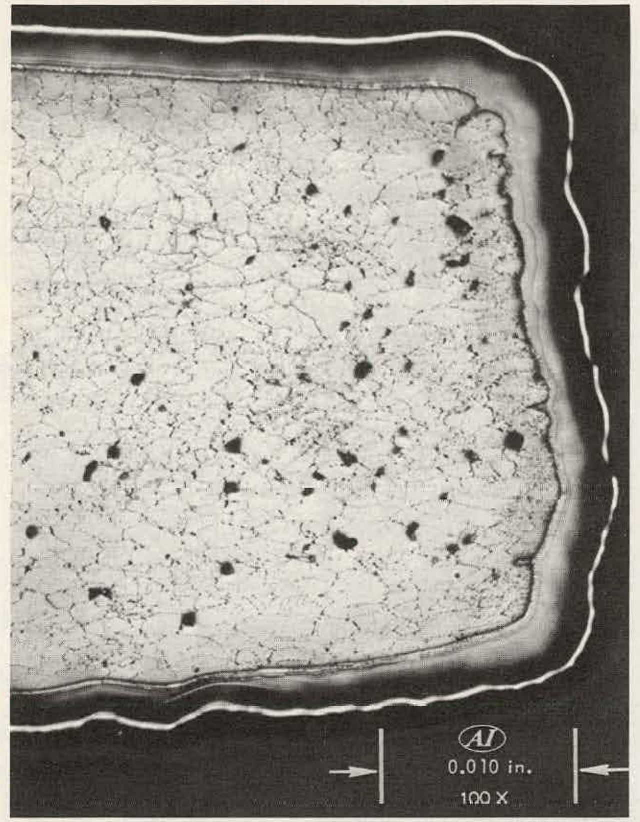

SN 2245

a. No Helium, Rupture Life = 1075 hr, Elongation = 44%

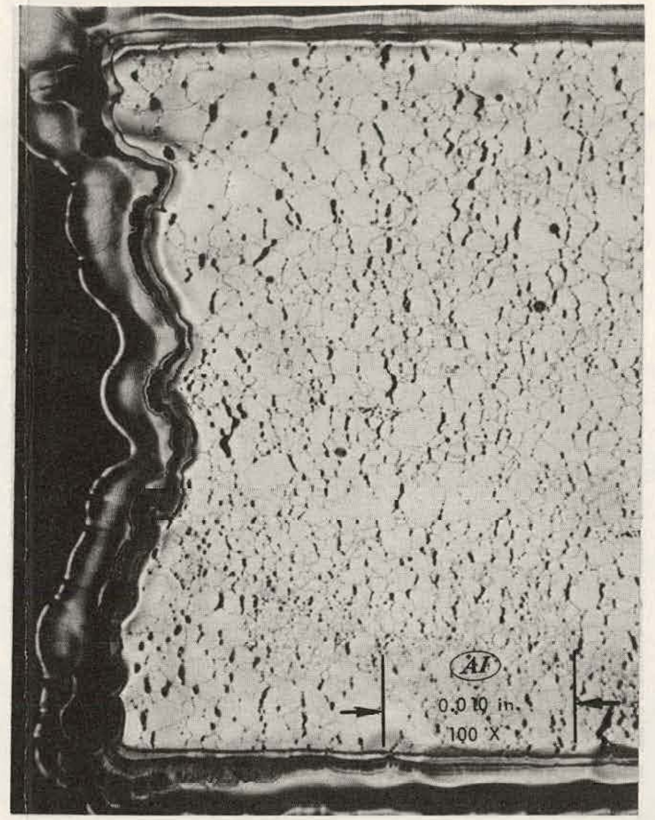

SN 2303

b. 4.0×10^{-5} atom fraction Helium, Rupture Life = 594 hr, Elongation = 10%

Figure 4. Type 316 Stainless Steel (Treatment 6) Tested at 700°C (Note increased intergranular cracking and lack of grain distortion in helium-containing sample, compared to control)

SN 2247

a. No Helium, Rupture Life = 683 hr, Elongation = 5%

SN 2248

b. 4.0×10^{-5} atom fraction Helium, Rupture Life = 173 hr, Elongation = 2%

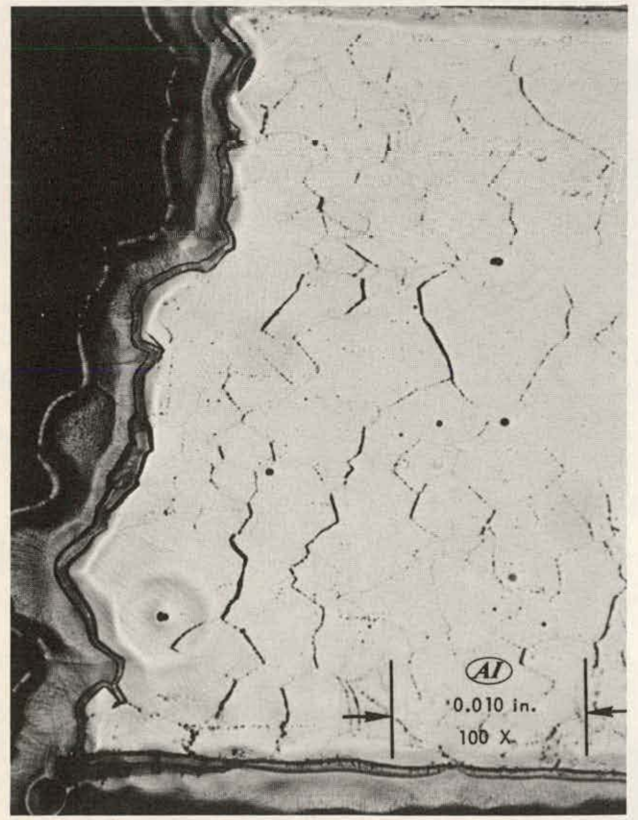

SN 2304

c. 4.0×10^{-5} atom fraction Helium, Rupture Life = 401 hr, Elongation = 1%

Figure 5.

Type 316 Stainless Steel (Treatment 13) Tested at 700°C (Note increase in intergranular cracking in helium-containing samples, and increased amount of multifaceted cracks in c., compared to b.)

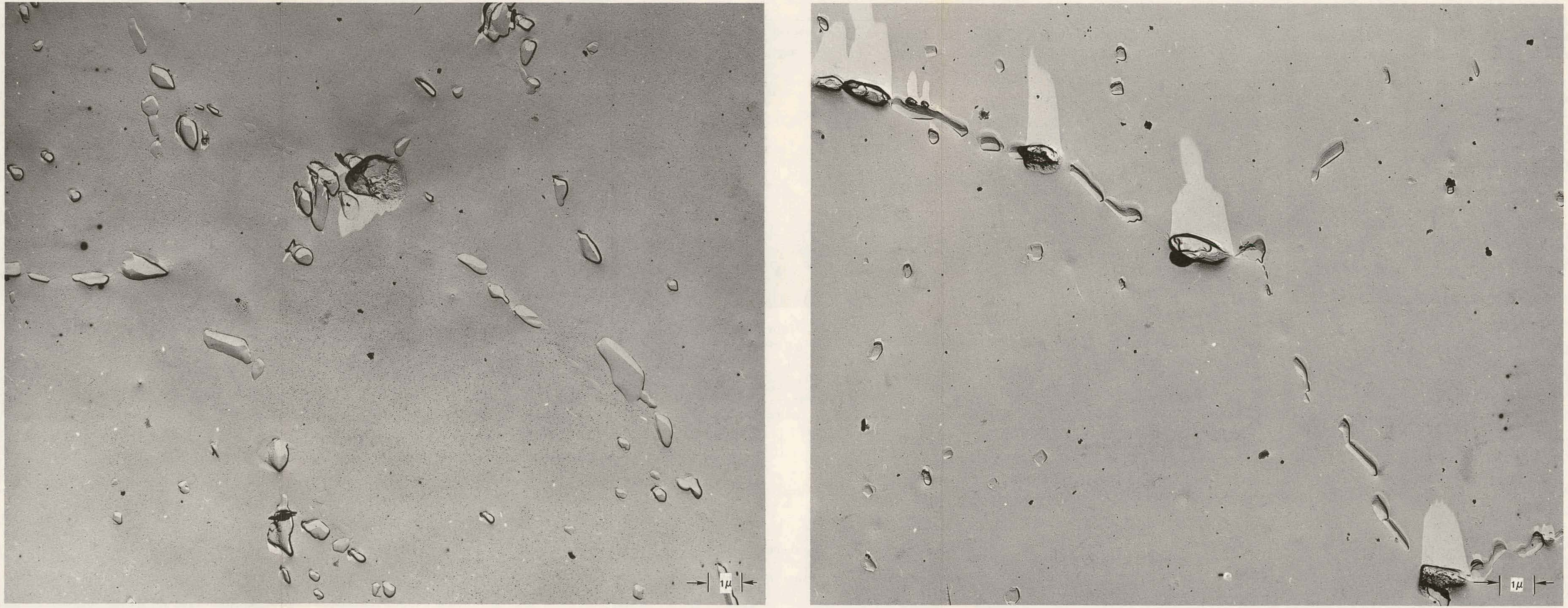

8719

a. No Helium, Rupture Life = 1075 hr, Elongation = 44%

8727

b. 4.0×10^{-5} atom fraction Helium, Rupture Life = 316 hr, Elongation = 13%

Figure 6. Type 316 Stainless Steel (Treatment 6) Tested at 700°C (Note increase in voids on grain boundaries of helium-containing sample over control)

The cracking in Type 316 (Treatment 13) samples appears to result from linking up of a number of small voids along the grain boundary. In the case of Sample 9-59 (Figure 5b), the cracks extend primarily over one grain facet or a fraction thereof, with only a few multifaceted cracks. In Sample 9-9 (Figure 5c), the number of multifaceted cracks is greater, as is the overall amount of cracking. These samples had rupture lives which occurred, respectively, before and after the break in the stress vs rupture life curve (Figure 2).

2. Replica Electron Microscopy

Replicas of Type 316 (Treatment 6 and Treatment 13) stainless steel are shown in Figures 6 and 7, respectively. These are two-stage replicas; therefore, the light shadow adjacent to a dark area indicates the position and size of a void. Samples of Type 316 (Treatment 6) and Type 304 had similar microstructures, and the following remarks also apply to the latter.

In almost all cases, the voids were located in the grain boundaries, adjacent to grain-boundary carbides. The number of voids per unit length of observed grain boundary was greater in the helium-containing samples.

3. Thin Foil Electron Microscopy

Figure 8 shows helium bubbles in Type 304 samples containing 1.5×10^{-6} and 3.5×10^{-5} atom fraction helium. The bubbles appeared in the matrix and in grain boundaries of both samples. The bubble size and density in the sample with the higher helium content is equivalent to that observed after tensile testing at the same temperature.(1)

Precipitation occurred during testing in the Type 316 (Treatment 6) control sample which had a life of 1075 hr. The precipitates, most of which could be identified by electron diffraction as σ-phase, nucleated on pre-existing carbides and in dislocation-cell walls.

Helium bubbles were observed at grain boundaries and within the grains in two of the three Type 316 (Treatment 6) helium-containing samples observed (Table 4). Figure 9 shows a string of helium bubbles along a grain boundary and in the matrix of Sample 9-15. Many of the bubbles in the matrix were attached to dislocations. Precipitation during testing occurred in Samples 9-5 and 9-72, but not in 9-15. Figure 10 shows a σ particle precipitated on an

$M_{23}C_6$ particle in Sample 9-72. The size and density of the new precipitates were greater in Sample 9-72 than in 9-5. Conversely, the helium bubble size and density are greatest in Sample 9-15, are less in 9-5, and are not detectable in 9-72.

In Type 316 stainless steel (Treatment 13) samples, the formation of new precipitates could not be determined due to the large amount of precipitation which had taken place during the pre-irradiation aging treatment. Figure 11 shows helium bubbles in the matrix, and in prior slip and deformation bands of the sample.

C. STRAIN ANALYSIS

A strain analysis was done on samples of Type 316 (Treatment 6), using Equation 1. The results are presented in Table 5, along with the overall strain. The strain due to cracking in the samples was obtained by drawing five lines, randomly spaced across the width of the photomicrograph, and measuring the width of the cracks parallel to the tensile axis. The total width of the cracks was then normalized to the total gauge length of the sample, and the strain calculated. This type of calculation was possible because the cracking was along the whole gauge length, and in a more or less uniform amount.

TABLE 5

SUMMARY OF STRAIN ANALYSIS ON STRESS-RUPTURE SAMPLES OF TYPE 316 STAINLESS STEEL GIVEN HEAT TREATMENT NO. 6 AND TESTED AT 700°C

Sample	Stress to Failure		Strain Measured on Traveling Microscope (%)	Slip Strain From Grain Analysis* (%)	Strain From Measuring Crack Thickness* (%)
	Stress (kpsi)	Time (hr)			
Control	12.0	1075	44 ± 2	47 ± 3	
Helium	10.9	594	10 ± 2	3 ± 2	9 ± 1

*The limits given are the most probable error.

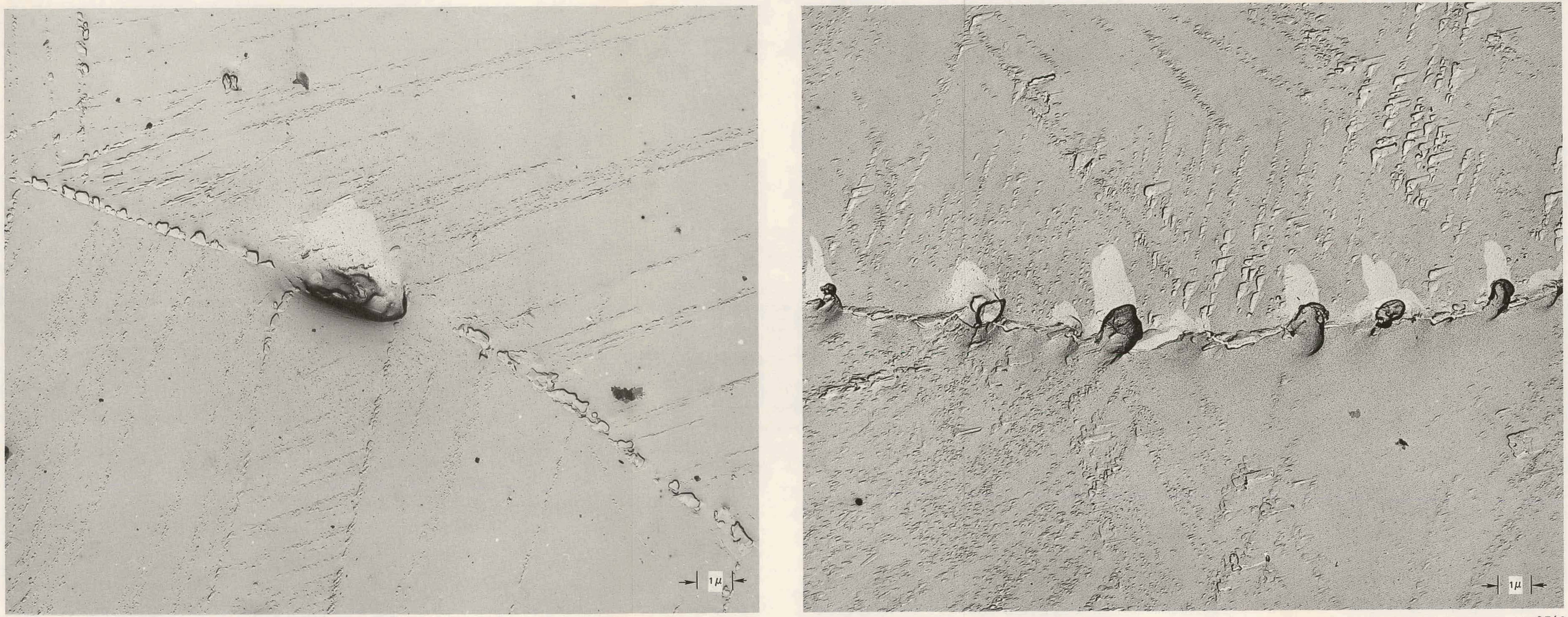

8731

a. No Helium, Rupture Life = 683 hr, Elongation = 5%

8761

b. 4.0×10^{-5} atom fraction Helium, Rupture Life = 173 hr, Elongation = 2%

Figure 7. Type 316 Stainless Steel (Treatment 13) Tested at 700°C (Note increase in voids on grain boundaries of helium-containing sample)

7889

a. 1.5 x 10^{-6} atom fraction Helium, Rupture Life = 419 hr, Elongation = 17%

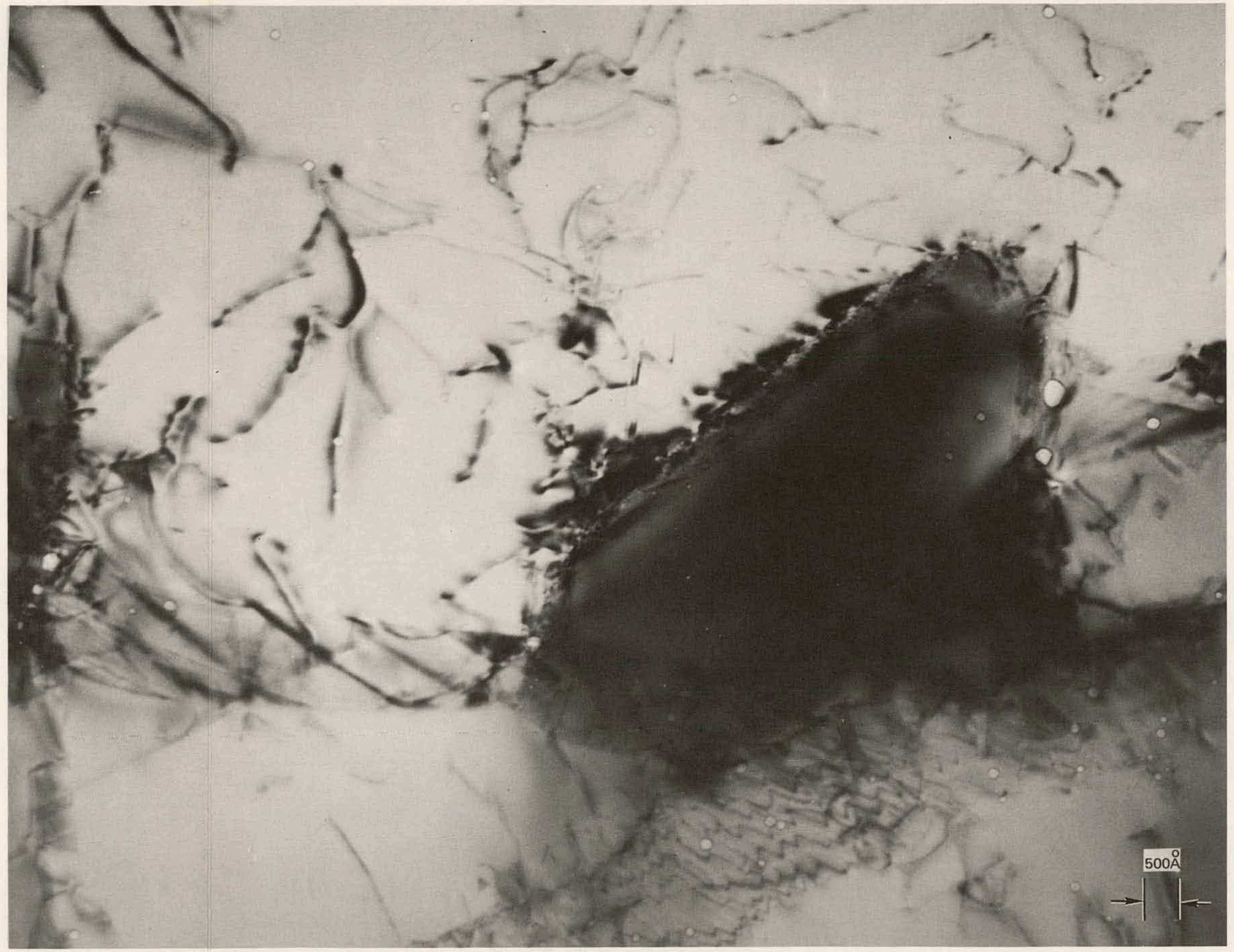

7822

b. 3.5 x 10^{-5} atom fraction Helium, Rupture Life = 325 hr, Elongation = 11%

Figure 8. Type 304 Stainless Steel Tested at 760°C (Largest helium bubbles are generally in carbide-matrix interface)

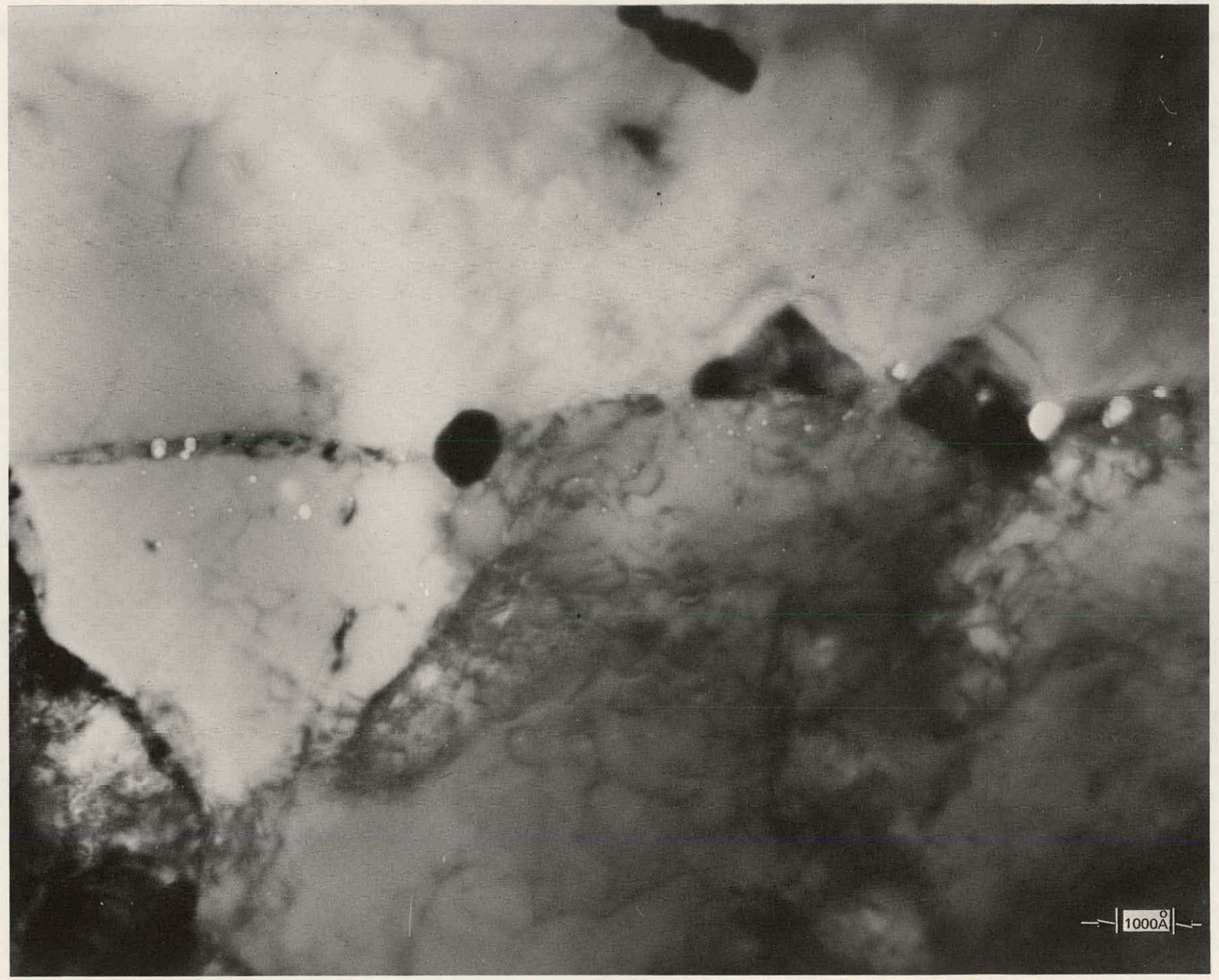

8866

Figure 9. Type 316 Stainless Steel (Treatment 6) Containing 4.0×10^{-5} atom fraction Helium, Tested at 700°C, Showing Helium Bubbles in Grain Boundary.
Rupture Life = 316 hr, Elongation = 13%

8043

Figure 10. Type 316 Stainless Steel (Treatment 6) Containing 4.0×10^{-5} atom fraction Helium, Tested at 700°C, Showing Growth of Sigma Phase on $M_{23}C_6$ Particle.
Rupture Life = 594 hr, Elongation = 10%

8861

Figure 11. Type 316 Stainless Steel (Treatment 13) Containing 4.0×10^{-5} atom fraction Helium, Tested at 700°C, Showing Helium Bubbles in Matrix and in Prior Slip and Deformation Bands.
Rupture Life = 173 hr, Elongation = 2%

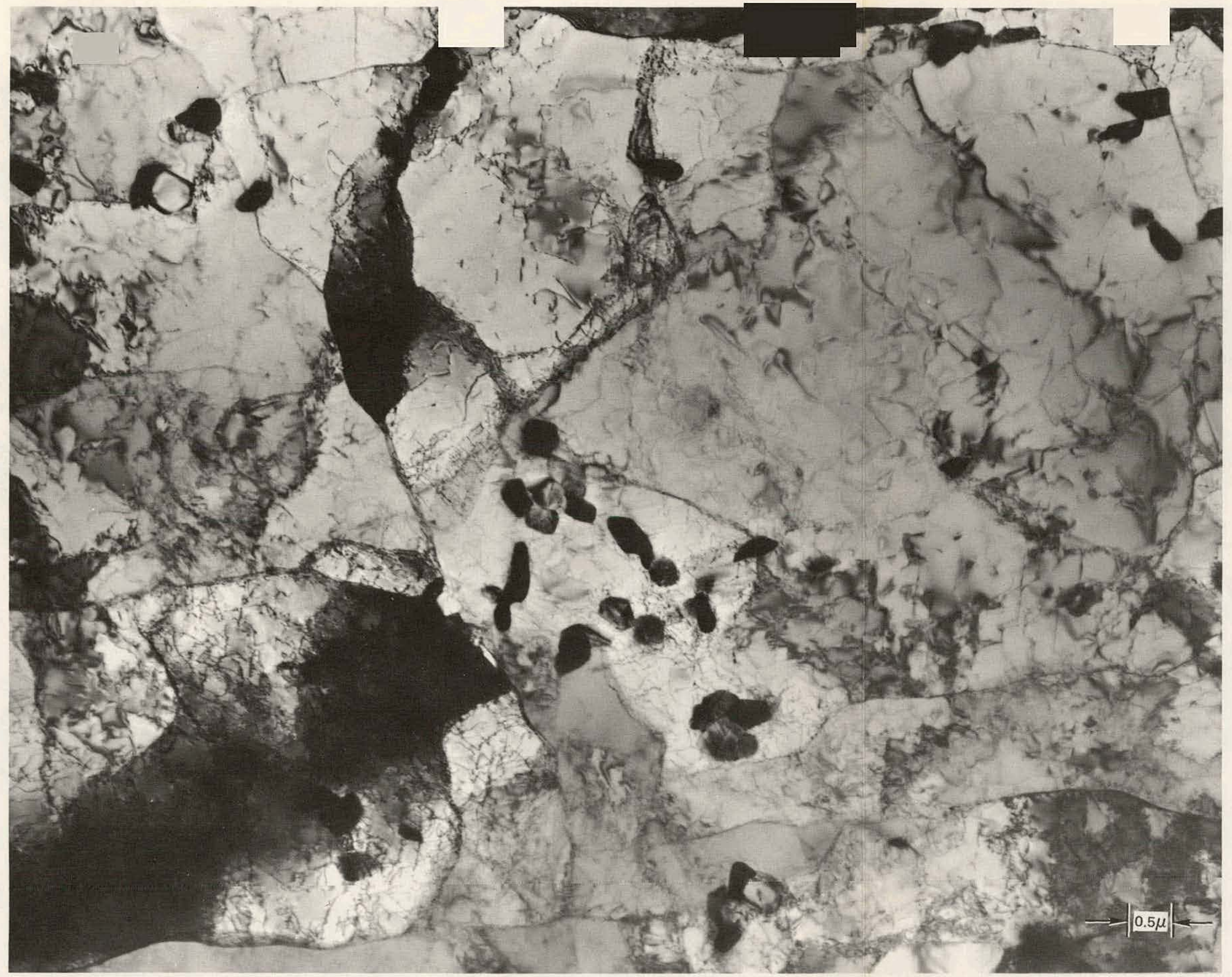

8823

a. No Helium, Rupture Life = 1075 hr, Elongation = 44%

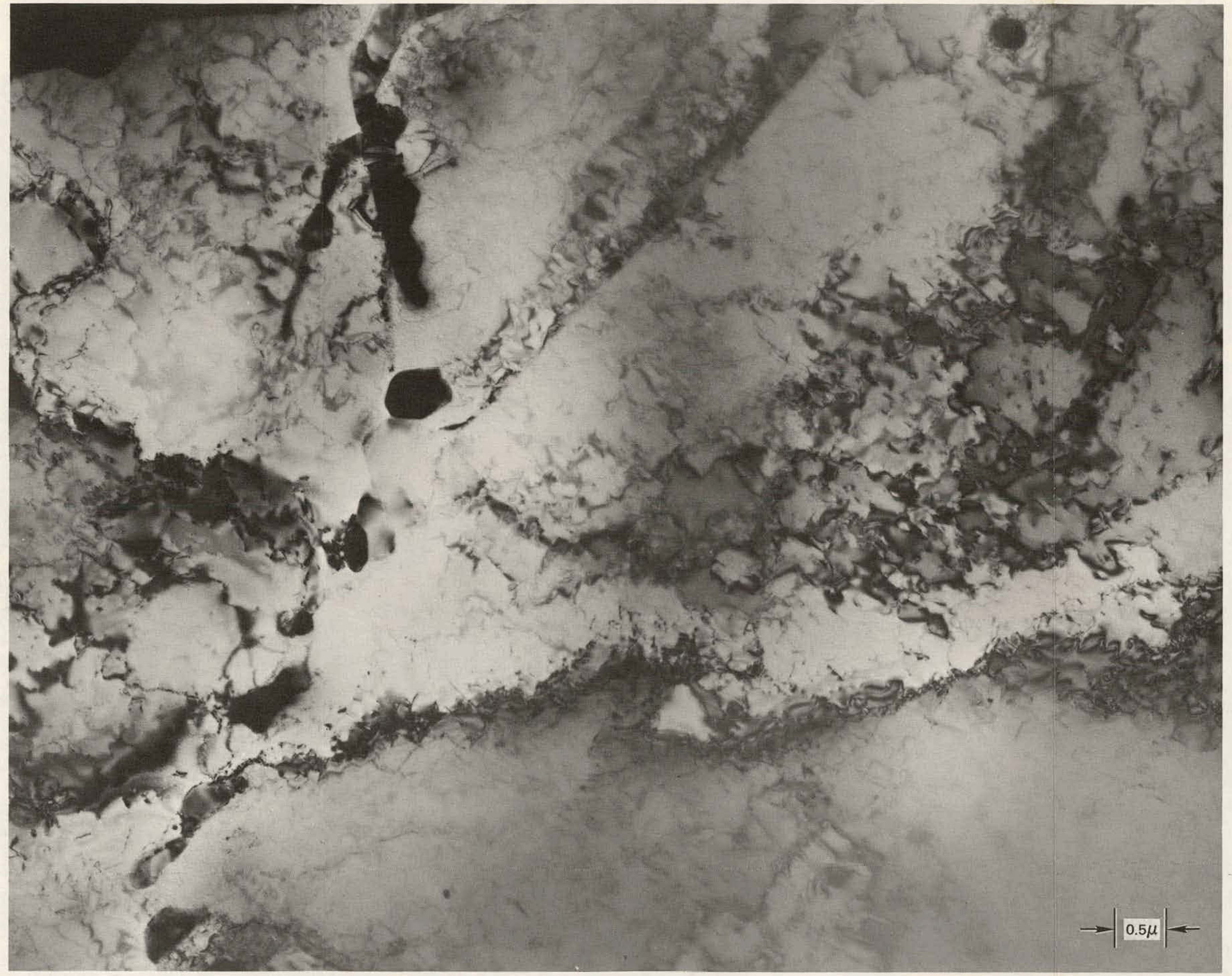

217

b. 4.0×10^{-5} atom fraction Helium, Rupture Life = 316 hr, Elongation = 13%

Figure 12. Type 316 Stainless Steel (Treatment 6) Tested at 700°C (Note lack of polygonization in helium-containing sample)

These results indicate that the strain which takes place in the control sample is entirely within the grain, whereas the internal strain in the helium-containing samples is only a small fraction of the measured elongation, the remainder being due to cracking.

This difference in the amount of strain taking place within the grains is reflected in the dislocation structure of the samples. Figure 12a is a transmission electron micrograph of the control sample, showing the typical dislocation arrangement, including polygonization. Figure 12b is a similar transmission electron micrograph of a helium-containing sample. Note that there is little, if any, polygonization in this case.

IV. DISCUSSION

Helium reduced the rupture life of Types 304 and 316 (Treatment 6) by a factor of 2 to 3 in the present work. This reduction compares with factors of 5 to 10, as reported for neutron-irradiated austenitic stainless steels.[8,9] When comparing these results, it is necessary to consider the distribution of helium in the microstructure, as well as the overall helium concentration.

If helium is produced mainly by the ^{10}B (n, α) ^{7}Li reaction with thermal neutrons, then the distribution of boron in the microstructure can exert an influence on the resulting helium distribution. Since boron is often concentrated at grain boundaries, high local helium concentrations may be expected there.[10,11] This could result in a degree of embrittlement much larger than would be the case, if the helium concentration were uniform throughout the microstructure.

Although the control samples of Type 316 (Treatment 13) exhibit better stress-rupture properties than the control samples given Treatment 6, it appears doubtful that the helium-containing samples will have a similar behavior. There is considerable loss in strength and rupture life above ~300 hr, as seen in Figure 2. Extrapolating the data to ~1000 hr indicates that Treatments 6 or 13 would result in about the same strength. Further extrapolation cannot be justified, in light of the data.

Even the Type 316 samples containing 1.5×10^{-6} atom fraction helium show a more pronounced effect at the longer times than do the solution-annealed samples. At 100 hr, there is no effect on strength or rupture life; however, at ~1000 hr, the loss in strength is about twice that of the material given Treatment 6 (~17% vs 9%).

From the metallographic examinations, summarized in Table 4, it appears that the basic mechanisms which were found to cause premature failure during tensile testing of these alloys[1,2] also operate during the stress-rupture or creep process. Aside from the increased intergranular cracking and the appearance of new precipitates which formed during testing, the metallographic observations are quite similar (i.e., intergranular cracks are initiated adjacent to grain-boundary carbides, helium bubbles are found in the matrix, generally associated with dislocations, and in the grain boundaries, where the larger bubbles are attached to carbide particles).

Also, in regard to the intergranular cracking, the qualitative observations of the light microscopy are reinforced by the quantitative indications of the strain analysis. These results (Table 5) show that the strain which takes place in control samples is almost entirely within the grains; whereas, in the samples containing helium, the measured elongation is primarily due to cracking of the sample, with only a small fraction of the strain taking place in the grains. There are two aspects of the calculation of E_c, the strain due to cracking, which must be discussed. First, the cracks appear wider than they actually are, because of etching effects during the metallographic preparation. This would tend to overestimate the amount of strain due to cracking. Second, the very narrow cracks were not measured, because of the difficulty in distinguishing them from the grain boundaries. This tends to underestimate the amount of strain due to cracking. We are not implying, from this discussion, that these errors compensate for each other and that the value of E_c given is exact, but that it is an indication of the relative amount of cracking when compared to the other strain measurements.

Barnes[12,13] originally proposed a model in which helium atoms and small bubbles diffuse to, and/or are swept by dislocations into, the grain boundaries. The helium is then confined to the plane of the grain boundary, where it agglomerates into larger bubbles. These larger bubbles, frequently found at the grain-boundary carbide-matrix interface, act as voids which open up during further deformation.

In the short times involved during tensile testing, strain is more imporant than diffusion below $\sim$800°C.[1] However, the situation may be different during stress-rupture testing. The copious amount of intergranular cracking observed in the samples, and the small amount of strain which apparently has taken place in the grains (see Figures 3, 4, and 5, and Table 5), can be interpreted in two ways. First, the small amount of strain produces a sufficient amount of helium in the grain boundaries to nucleate cracks, and further elongation takes place by the growth of the intergranular cracks. This implies that the strain within the grains is completed in the early stages of the deformation process.

The second possibility is that the strain within the grains, and crack nucleation and growth, occur throughout the test, and that the elongation due to cracking simply adds, incrementally, to the overall elongation. In both cases, cracking is extensive, leading to intergranular failure; at present, the available information is insufficient to resolve this point.

V. CONCLUSIONS

1) Helium reduces the rupture life and elongation of Types 304 and 316 stainless steels.

2) For the solution-annealed state, the reduction in rupture life, for times up to 1000 hr, is independent of the helium concentration between 1.5×10^{-6} and 4.0×10^{-5} atom fraction helium.

3) In cold worked and partially annealed Type 316 stainless steel, the reduction in rupture life is dependent on the helium concentration. For material with 1.5×10^{-6} atom fraction helium, the reduction in rupture life increases as the initial stress decreases. For material with 4.0×10^{-5} atom fraction helium, the reduction in rupture life is about constant, up to ~300 hr, after which the material drastically loses its creep strength.

4) The amount of strain which takes place within the grains of the helium-containing samples is a small fraction of the total elongation measured after testing. The remainder of the measured elongation is due to the intergranular cracking.

REFERENCES

1. D. Kramer, H. R. Brager, C. G. Rhodes, and A. G. Pard, J. Nuc. Mat. 25, 121 (1968); also "Helium Embrittlement in Type 304 Stainless Steel," NAA-SR-12601 (December 5, 1967)

2. D. Kramer, K. R. Garr, C. G. Rhodes, and A. G. Pard, J.I.S.I. 207, 1141 (1969); also "Helium Embrittlement of Type 316 Stainless Steel," AI-AEC-12670 (April 30, 1968)

3. H. Farrar IV and C. H. Knox, Trans. Am. Nuc. Soc. 11, 503 (1968)

4. W. A. Rachinger, J.I.M. 81, 33 (1952-53)

5. J. H. Hensler and R. C. Gifkins, J.I.M. 92, 340 (1964)

6. O. L. Davies, ed., Statistical Methods in Research and Production, 3rd ed. (Hafner Publishing Co., New York, 1958) p 51

7. A. G. Worthing and J. Geffner, Treatment of Experimental Data (John Wiley & Sons., Inc., New York, 1948) p 208

8. P. C. L. Pfeil and D. R. Harries, "Effects of Irradiation in Austenitic Steels and Other High Temperature Alloys," Flow and Fracture of Metals and Alloys in Nuclear Environments, ASTM STP 380, 202 (1965)

9. E. E. Bloom, "In-Reactor and Postirradiation Creep-Rupture Properties of Type 304 Stainless Steel at 650°C," ORNL-TM-2130

10. D. R. Harries, J. Brit. Nuc. Energy Soc. 5, 74 (1966)

11. A. F. Rowcliffe, G. J. C. Carpenter, H. F. Merrick, and R. B. Nicholson, "An Electron Microscope Investigation of High-Temperature Embrittlement of Irradiated Stainless Steel," Effects of Radiation on Structural Metals, ASTM STP 426, 161 (1967)

12. R. S. Barnes, "Mechanisms of Radiation-Induced Mechanical Property Changes," Flow and Fracture of Metals and Alloys in Nuclear Environments, ASTM STP 380, 40 (1965)

13. R. S. Barnes, Nature 206, 1307 (1965)